Model based design of an intercooled dual stage sliding vane rotary compressor system

Roberto Cipollone[1], Giuseppe Bianchi[1], Davide Di Battista[1], Giulio Contaldi[2], Stefano Murgia[2]

[1]Department of Industrial and Information Engineering and Economics, University of L'Aquila, L'Aquila, Italy
[2]Ing. Enea Mattei S.p.A, Vimodrone (Milan), Italy

E-mail: roberto.cipollone@univaq.it

Abstract. Energy saving is currently one of the most important driving factors for innovation all over the world. With reference to global electricity consumptions, electrical energy for compressed air production accounts for 4-5%. Among the rotary compressor technologies, Sliding Vane Rotary Compressors (SVRC) are characterized by noteworthy specific energy consumptions and demonstrated an unforeseen energy saving potential thanks to some intrinsic features specifically related to this kind of machines. The paper presents a further reduction strategy to lower energy consumptions in compressed air systems using SVRCs that relies on the combination of the recent use of a pressure swirled oil injection technology and a dual stage intercooling. The synergy between technologies already mature approaches to the lowest energy consumption and candidates SVRCs as superior machines in the energy context. The saving potential compared to the technology at the state of the art was evaluated thanks to a comprehensive mathematical modeling of the two compressor sections and the intercooling heat exchanger and fan. Results showed a reduction of the electrical power required to drive the compressor system up to 9.5%. The overall approach represents a model-based design for a new machine which is under development.

1. Introduction

Compressed air is an indispensable utility for industrial processes that is almost exclusively produced by electric energy and accounts for 10-15% of overall electricity consumption in the industrial sector [1, 2]. In particular, Figure 1 shows that the most energy consumer are machines in the range of 10-30 m^3/min [3]. Furthermore, if compressed air production for commercial and residential markets is taken into account, the overall consumptions would reach 20% [4]. Energy saving in Compressed Air Systems (CAS) might be accomplished through interventions upstream and downstream the compressor. Among them, compressor technology and operation belong to the first category and they account for a consumption share close to 10-20% [2].

In order to compare energy consumptions of current industrial air compressors and to outline suitable future improvement strategies, the Authors developed a procedure to define homogeneous operating points starting from energy consumptions at given operating conditions for different compression technologies and manufacturers provided in CAGI's datasheets [3]. Among the performance indicators, the global compressor efficiency, whose mathematical formulation is reported in Equation 1, not only depends on the compressor but also on its auxiliaries and electric motor [5].

Content from this work may be used under the terms of the Creative Commons Attribution 3.0 licence. Any further distribution of this work must maintain attribution to the author(s) and the title of the work, journal citation and DOI.
Published under licence by IOP Publishing Ltd

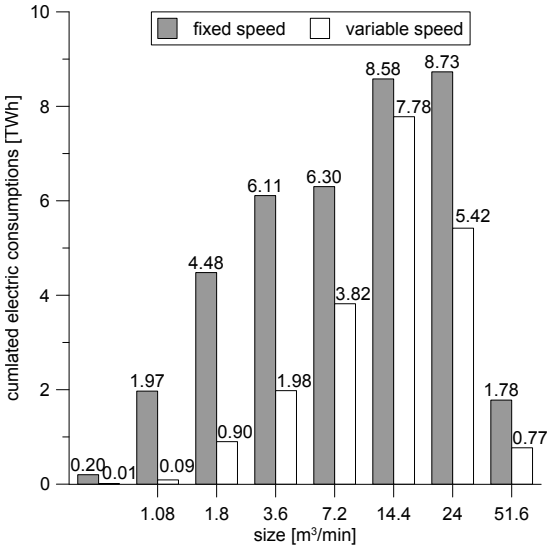


Figure 1: Cumulated electric energy consumption distribution per compressor size

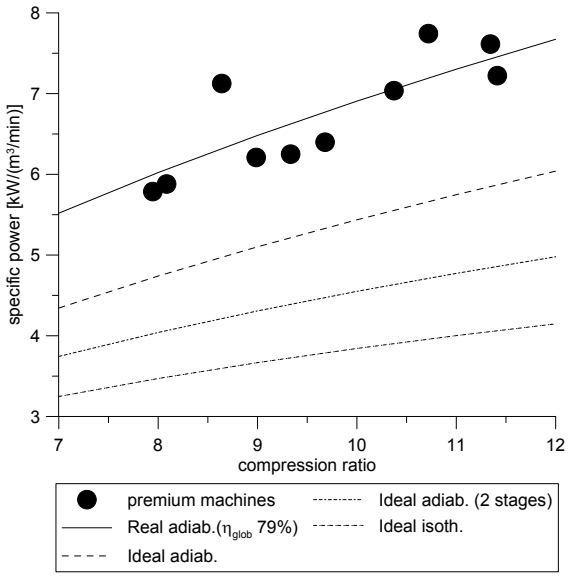


Figure 2: State of the art and goals for the energy saving in compressed air systems

$$\eta_{glob} = \eta_{vol}\,\eta_{ad-is}\,\eta_{mech}\,\eta_{org}\,\eta_{el} \tag{1}$$

The investigation carried out is summarized in Figure 2 and states that real performances of current premium machines closely fit a global compressor efficiency of 79%. Although improvements can still be accomplished, electric and mechanical technologies have reached a good level of development. Therefore, a great saving potential is mainly achievable on the thermodynamic side. The theoretical analysis reported in Figure 2 also reports ideal performances for adiabatic-isentropic and isothermal transformations. The latter trend could be achievable with infinite intercooled stages. However, almost half of the saving potential associated to a transition from an adiabatic-isentropic to an isothermal compression could be reached just with a dual stage compressor system. These general predictions were calculated disregarding the effects that mechanical and organic losses (fan consumption) have on the energy consumptions.

To address the energy saving strategy identified towards an industrial product, the paper presents a model based design of a dual stage intercooled compression system. The compressor technology taken as reference is the sliding vane rotary one. In literature, research was carried out through modeling and experimental approaches aiming at investigating the intrinsic features that belong to this kind of machines. These analyses provided relevant information concerned to the vane dynamics [6, 7], friction phenomena [8, 9], leakage between vanes [10, 11, 12] as well as methodologies that allowed to measure the vane pressure evolution in order to estimate the compressor performance [13, 14]. Even if the development of dual stage compressor prototypes was previously investigated for air conditioning applications [15, 16, 17], those machines were small scale ones ($< 1kW/(m^3/min)$). Hence, according to Figure 1, they would not lead to noticeable energy saving benefits in CAS in global terms. On the other hand, some researchers developed a model based design of a dual stage sliding vane rotary compressor system using a unique rotor [18]. Nevertheless, this theoretical concept might have drawbacks in terms of technical and economical feasibility of a real prototype because of sealing and stability issues for the compressor blades while sliding along stators with different curvature.

2. Design Methodology

In previous experimental studies on single stage sliding vane compressors, vane pressure was measured and allowed the reconstruction of the indicator (pressure-volume) diagram of the machine. These activities revealed that current sliding vane technology is characterized by a closed-volume compression transformation that follows an adiabatic trend [19]. Since minimum work occurs for an isothermal compression, to approach the lowest energy consumption, the innovative compressor design proposes to split the compression ratio in two stages, cooling the compressed air in between (Figure 3).

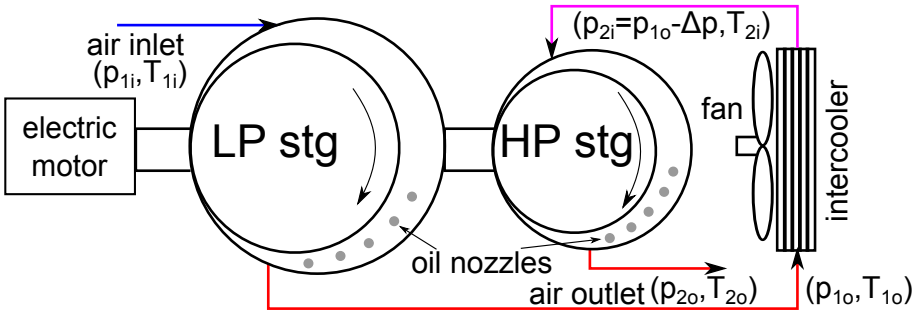


Figure 3: Dual compression stage with internal and intermediate air cooling

From technical and economic viewpoints, the best trade-off in terms of energy saving and feasibility of the technology resulted in a system layout with two compressors. In a dual stage compression, the compression ratio that minimizes the input work is ideally the square root of the total pressure ratio. However, in case of a real intercooler, a temperature difference between the compressed air at the heat exchanger outlet and the environment must exist. Hence, the intermediate pressure that minimizes the overall compression work can be analytically evaluated according to Equation 2.

$$p_{2i} = \sqrt{p_{1i}\, p_{2o} \left(\frac{T_{2i}}{T_{1i}}\right)^{\frac{\gamma}{\gamma-1}}} \tag{2}$$

In the current design approach, air is not only cooled during the passage from the Low Pressure (LP) stage to the High Pressure (HP) one, but also along both the compression processes thanks to an innovative oil sprayed injection technology whose features are presented in the following paragraph. Since both the machines were supposed to be driven by the same electric motor (i.e. same revolution speed), the HP compressor resulted smaller than the LP one. As concerns the air to air intercooler, a fan was needed to enhance the heat transfer. The energy consumption of this device was eventually discounted from the energy benefits achieved.

3. Compressor Model

The design of the dual stage sliding vane compressor was supported by a comprehensive simulation platform that is able to reproduce performances of real machines and to explore new design configurations. The model is composed of different modules that interact together according to the scheme reported in Figure 4. The mathematical model takes into account all the main physical phenomena occurring in sliding vane compressors [19, 20]. The vane filling and emptying processes were modeled through a one-dimensional quasi-propagatory approach. The parametric geometry modelling allows to investigate sliding vane machines (compressors and expanders) with any suction and discharge ports layout, both axial and radial. The blade dynamics module solves the Newton's 2nd of motion and the hydrodynamic lubrication at the blade tip which is the most severe location for friction losses.

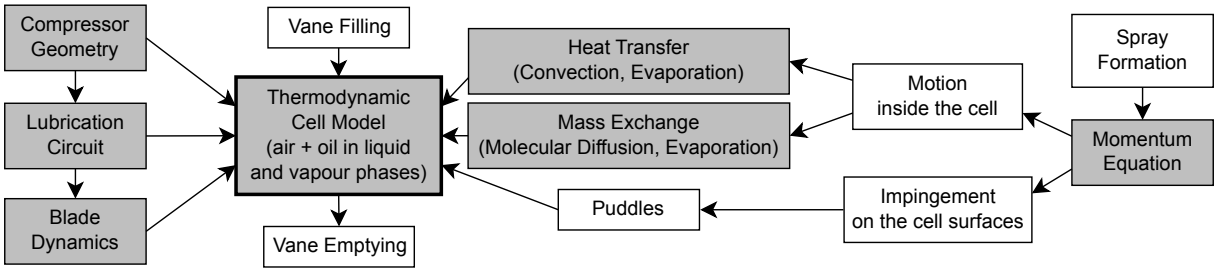


Figure 4: Compressor model block diagram

As concerns the lubrication circuit, two configurations may be studied: a conventional one, whereas oil is supplied through calibrated holes as liquid jets, and an innovative sprayed injection technique that relies upon atomizers to enhance the heat transfer between oil and air. The sprayed injection technique was modeled with a Lagrangian approach and applies conservation equations to oil particles after the spray break-up: downstream the break-up length, the Rosin Rammler oil droplet size distribution is discretized into parcels that, travelling along the compressor vane while it rotates, absorb heat from the compressing air until the impingement on the cell surfaces is reached and puddles build up. As shown in Figure 4, the core of the compressor model is the thermodynamic cell module that collects all the energy input and output fluxes to determine the pressure inside the compressor cells.

The mathematical model has been extensively validated both for the conventional and innovative oil injection techniques through experimental campaigns on industrial sliding vane compressors at different operating points (delivery pressure, revolution speed, etc.) [19, 21, 22]. The comparison between experimental and simulated indicator diagrams stated the accuracy and reliability of the model. Additional details on the modelling and experimental activities that led to the development of the compressor simulation platform can be found in the references [19, 20, 23, 24].

4. Intercooler Model

The benefits of splitting the overall compression ratio in two separate stages are strictly related to the chance of cooling the compressed air in between. To predict the air temperature at the inlet of the HP stage and pressure drops due to the intercooler, a mathematical model of the heat exchanger was developed relying on the know-how acquired on engine cooling circuit modeling [25]. Furthermore, an axial fan was considered to force the cooling air crossing the heat exchanger.

4.1. Heat Exchanger

Air-to-air heat exchangers that are commonly used in industrial applications are the tube and fin type because of high heat transfer rates and relatively low pressure drops. In these devices, the hot stream (compressed air) flows in circular tubes externally finned and it is cooled by ambient air pushed by a fan. After a preliminary design that estimated a suitable size and geometry of the intercooler, the heat exchanger was modeled through a one-dimensional approach, dividing it in a series of elementary ducts. For each of them, conservation equations are solved in a simplified way, in order to evaluate the thermal power exchanged, pressure drops and the resulting outlet flows conditions. To compute the thermal power exchanged in each elementary duct, an electrical analogy was used: as shown in Figure 5, a series of heat transfer resistances was considered. In particular a forced convective resistance was used between the compressed air and the internal tube wall while a conductive resistance was adopted between the metallic tube walls. The presence of fins on the external wall of the tube eventually led to an enhanced forced

convection with ambient air. Thermal resistances were evaluated considering the elementary heat exchanger geometry and the convective heat transfer coefficients according to Nusselt correlations. Mathematical formulations are reported in Equations 3 and 4 while symbols explanation are given in the nomenclature. The elementary thermal power exchanged was calculated considering the temperature difference between internal and external values according to Equation 5.

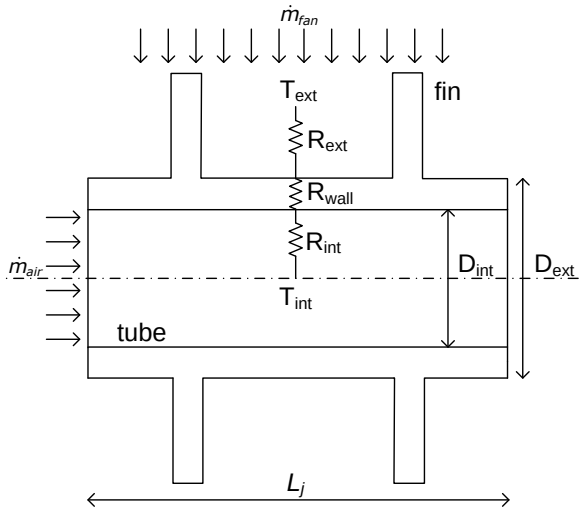


Figure 5: heat exchange model of an elementary duct

$$R_{int} = \frac{1}{h_{int}\, S_{int}} \qquad (3)$$

$$R_{wall} = \frac{ln(D_{ext}/D_{int})}{2\pi\, k\, L_j}$$

$$R_{ext} = \frac{1}{h_{ext}\, S_{ext}}$$

$$Nu = C \left(\frac{\dot{m}}{\mu\, A}\, L_j \right)^n Pr^{1/3} \qquad (4)$$

$$Q_j = \frac{T_{int} - T_{ext}}{R_{int} + R_{wall} + R_{ext}} \qquad (5)$$

Pressure drops are evaluated considering friction between fluids and heat exchanger walls according to the corrected Darcy correlation reported in Equation 6:

$$\Delta p = f_m \frac{32\, \mu\, v}{D^2{}_{wet}}\, L_j \qquad (6)$$

where the wet diameter D_{wet} corresponds to the inlet diameter at the inner tube side and to the diameter of the equivalent duct between two fins at the outer side. The correlation also takes into account a suitable friction multiplier f_m in both sides of the heat exchanger.

4.2. Fan Model

The mass flow rate of cooling air is calculated solving the model of an electrical axial fan. At a given revolution speed taken as reference, the fan operating curve (pressure increase vs. flow rate) was evaluated according to Equation 7.

$$\dot{V}(N_{ref}) = \dot{V}_{max} - \alpha \left(\frac{p_o}{p_i} - 1 \right)^2 \qquad (7)$$

The latter expression required the knowledge of an operating point (e.g. design point) and the maximum flow rate $\dot{V}_{max}$ (which corresponds to a nil pressure increase). Operating curves at different revolution speeds were retrieved using a similarity law with respect to reference conditions (Equation 8).

$$\dot{V}(N) = \dot{V}(N_{ref}) \frac{N}{N_{ref}} \left(\frac{p_o}{p_i} - 1 \right) = \left(\frac{p_{o,ref}}{p_{i,ref}} - 1 \right) \left(\frac{N}{N_{ref}} \right)^2 \qquad (8)$$

Electrical power required to drive the cooling air through the heat exchanger was evaluated using Equation 9 that assumed a product between mechanical and electrical efficiencies of 20%.

$$P_{el,fan} = \frac{\rho \dot{V} (p_o - p_i)}{0.2} \tag{9}$$

5. Results and discussion

The energy saving potential of a dual stage intercooled compression was assessed simulating different compressors system layouts and injection technologies. With reference to Figure 1, the analysis was carried out designing a compressor system in the most significant flow rate range for cumulated energy consumptions (23 m^3/min). Suction conditions were the ISO 1217 ones (1 atm and 20 $°C$) while the delivery pressure was set to 9 bar. A further parameter of investigation was the effectiveness of the intercooling process in terms of inlet temperature of the second stage (T_{2i}). In simulation cases A, B, C oil injection was performed in the conventional way, at only one angular location. Conversely, a series of five pressure-swirl nozzles were equally distributed along the compression process in cases D, E, F and supplied the same amount of lubricant of cases A, B, C respectively. Injection temperature was set to 40 $°C$ everywhere while injection pressure was equal to the discharge pressure of each compressor stage, as noticed experimentally [24].

Simulations data reported in Table 1 present a full energy breakdown of the compressor system: since sliding vane types are high-side compressors, according to Equation 10, in each machine mechanical power is not only needed to accomplish the compression process and to overcome friction losses but also to pressurize the oil that is injected in the compressor cells.

$$P_{mech} = P_{ind} + P_{fr} + P_{oil} \tag{10}$$

$$\eta_{glob} = P_{ind}/P_{el} = \eta_{el}\, P_{ind}/P_{mech} = \eta_{el}\, \eta_{mech} \tag{11}$$

Compression power was eventually calculated from the area of the indicator diagram according to the methodology proposed in [19]. Package power, i.e. the electrical power needed to drive the compressor system and the intercooler fan (if present), was computed assuming an IE2 efficiency class for 4-poles electric motors operating at 50 Hz. This choice fixed the revolution speed of all compressors to 1500 RPM. However, since the efficiency of the electric motor increases with its size, the comparison was made in terms of mechanical power rather than the electrical one. Furthermore, since in SVRCs oil pressurization is accomplished without an auxiliary device, the mechanical efficiency reported in Equation 11 also takes into account organic losses. Figure 6 compares indicator diagrams of single stage compressor with conventional (case A) and innovative oil injection technology (case D). The internal air cooling accomplished by oil droplets would bring the adiabatic compression phase towards an isothermal trend, with a potential saving in the indicated power close to 3 kW. Since compressor geometry and operating parameters of the lubrication circuit (injection pressure and flow rate) were kept constant, friction losses and oil pressurization power would not change. This fact motivates the slight decrease of the mechanical efficiency in case D.

Figure 7 reports indicator diagrams related to a typical intercooled dual stage configuration. When the compression process is split in two steps, at the LP compressor outlet air is at high pressure. Furthermore, assuming that oil is separated from air downstream each stage, because of the heat transfer with oil and metallic surfaces of the machine, air temperature at the compressor outlet would be at a value much lower than the one it would have had inside the compressor cell before the discharge. With reference to previous experimental campaigns, assuming that at the compressor exit air and oil have the same temperature T_o, this outlet value can be calculated according to Equation 12 in which variations of the specific heat at constant pressure for air and oil have been neglected since they are lower than 1.5%.

$$\dot{m}_{air}\, c_{p,air}(T_o - T_{air,i}) + \dot{m}_{oil}\, c_{p,oil}(T_o - T_{oil,i}) = P_{mech} \tag{12}$$

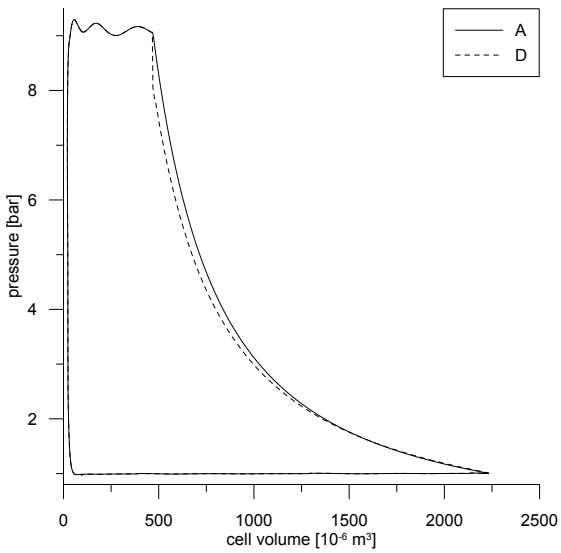


Figure 6: Single stage indicator diagram

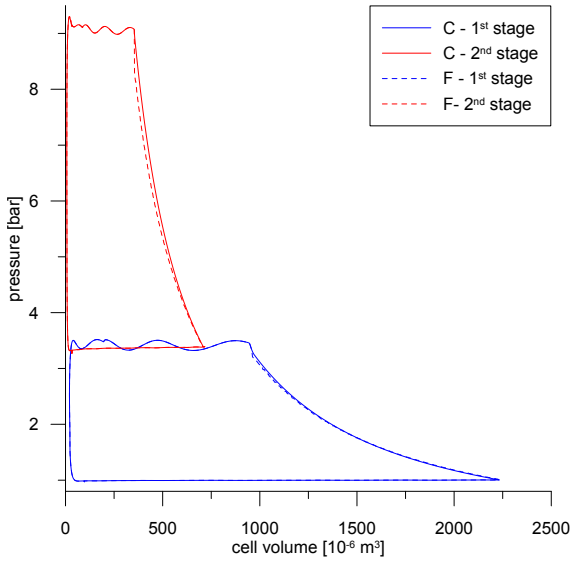


Figure 7: Dual stage indicator diagram

The resulting high fluid density would allow to reduce the volumetric capacity $\dot{V}_{air,2}$ of the HP compressor that would become more compact. In this way, friction losses could be reduced and the mechanical efficiency of the HP compressor would increase beyond 80%. Depending on the compressed air temperature at HP compressor inlet, the overall compression ratio was divided according to Equation 2 to achieve the optimal theoretical value of intermediate pressure. In simulation cases B and E, no intercooling was considered ($T_{2i} = T_{1o}$). On the other hand, in cases C and F air was further cooled up to 40 $°C$. Hence, the inlet temperature at the HP compressor got close to the ideal value ($T_{2i} = T_{1i}$) and reduced the difference between the compression ratios of the two stages. In order to keep the same machine geometry and its influence on friction losses between simulation cases B, C, E, F, optimal compression ratio was achieved tuning the angular displacement of the discharge ports. Simulations in Table 1 show that through a dual stage compression overall indicated power would decrease from 121.7 kW to 107.1 kW without intercooler and up to 104.4 kW with intercooler. These results are in agreement with the theoretical predictions reported in Figure 2 which compare specific compression powers of single and dual stage machines only from a pure thermodynamic point of view, i.e. without taking into account mechanical, organic and volumetric losses. However, since oil atomization depends on injection pressure, in case of dual stage compression the benefits of a sprayed injection technology would be less remarkable compared to the single stage process. This issue would be particularly critical for the first stage, whereas an injection pressure around 3.5 bar would not be able to properly atomize the oil jets. The resulting compression trend would be equal to an adiabatic one, as shown by the tendency of solid and dashed lines in Figure 7 to overlap. On the other hand, for the same lubrication circuit layout and overall oil flow rate, the compression split also divides the flow rate and injection pressure depending on the intermediate pressure value. Anyway, this results in a remarkable reduction of the pressurization power which accounts for 2.5 kW, as the energy saving that would be achived using the intercooling heat exchanger. Moreover, the first compression stage has the same geometry of the single stage compressor but accomplishes a lower indicated work to pressurize the air to 3 bar (instead of 9). Therefore, its mechanical efficiency results in very low values that consequently affect the mechanical efficiency of the whole compressor system. For these reasons, the 15% saving in terms of indicated power reduces to 9.5% with reference to electrical power.

Table 1: Simulations parameters and results
(p_{1i} 1 bar_a, T_{1i} 20.0°C, p_{2o} 9 bar_a, 1500 RPM)

case	A	B	C	D	E	F	
stages\spray\intercooling	1\N\N	2\N\N	2\N\Y	1\Y\N	2\Y\N	2\Y\Y	
$\dot{V}_{air,1}$	23.0	23.0	23.0	23.0	23.0	23.0	m^3/min
$\dot{V}_{air,2}$		7.1	7.4		7.1	7.4	m^3/min
$\dot{V}_{oil,1}$		148.0	129.4		148.0	129.4	L/min
$\dot{V}_{oil,2}$		148.1	170.9		148.1	170.9	L/min
$\dot{V}_{oil}$	303.9	296.1	300.3	303.9	296.1	300.3	L/min
$p_{1o} = p_{2i}$		3.7	3.4		3.7	3.4	bar_a
T_{1o}		55.5	56.3		55.5	56.3	°C
T_{2i}		55.5	40.0		55.5	40.0	°C
T_{2o}	81.0	46.1	45.6	81.0	46.1	45.6	°C
$P_{ind,1}$		62.6	57.0		62.3	56.8	kW
$P_{ind,2}$		44.5	47.4		43.3	46.2	kW
P_{ind}	121.7	107.1	104.4	118.7	105.6	103.0	kW
$P_{fr,1}$		26.3	26.3		26.3	26.3	kW
$P_{fr,2}$		7.3	7.4		7.3	7.4	kW
P_{fr}	27.3	33.6	33.7	27.3	33.6	33.7	kW
$P_{oil,1}$		0.9	0.9		0.9	0.9	kW
$P_{oil,2}$		1.6	1.9		1.6	1.9	kW
P_{oil}	5.1	2.5	2.8	5.1	2.5	2.8	kW
$P_{mech,1}$		89.8	84.2		89.5	83.9	kW
$P_{mech,2}$		53.4	56.7		52.2	55.5	kW
P_{mech}	154.0	143.3	140.9	151.1	141.7	139.4	kW
$\eta_{mech,1}$		69.7	59.2		69.6	67.6	%
$\eta_{mech,2}$		83.4	83.6		83.0	83.2	%
η_{mech}	79.0	74.8	74.1	78.6	74.5	73.8	%
P_{el}	162.3	151.0	148.5	159.2	149.4	146.9	kW

The intercooler design led to a heat exchanger made by aluminium with an internal heat exchange surface of 20 m^2 and a finned external one of 32 m^2. As shown in Figure 8, thermal performances are strictly related to mass flow rate of the cooling air which in turn depends on the fan revolution speed. In particular, cooling flow rate results from the equilibrium of the fan performance curves and the aeraulic pressure drop due to the heat exchanger (Figure 9). In cases C and F the thermal power exchanged in the intercooler is about 7.5 kW through an external air flow rate of 1200 m^3/h. At this operating point, fan would rotate at 1200 RPM and lead to a pressure rise of the cooling air around 30 Pa. On the other hand, pressure drops of the compressed air flow through the internal side of the intercooler would be close to 70 mbar. Fan electrical power absorbed would be eventually equal to 40 W. However, since the presence of this heat exchanger does not lead to significant efficiency improvements, in a future industrialization

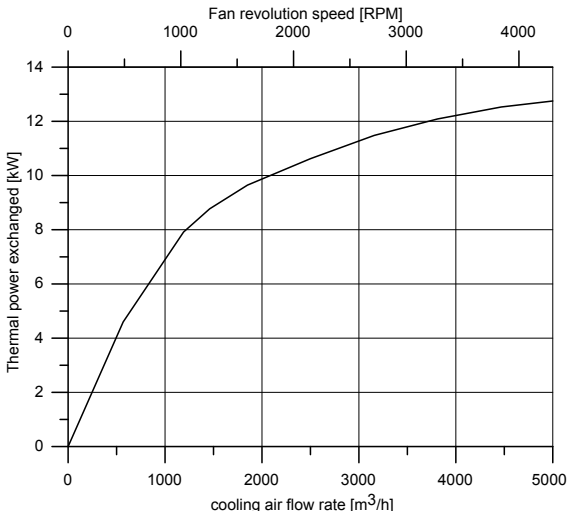


Figure 8: Influence of cooling mass flow rate (fan revolution speed) on the thermal power exchanged at the intercooler

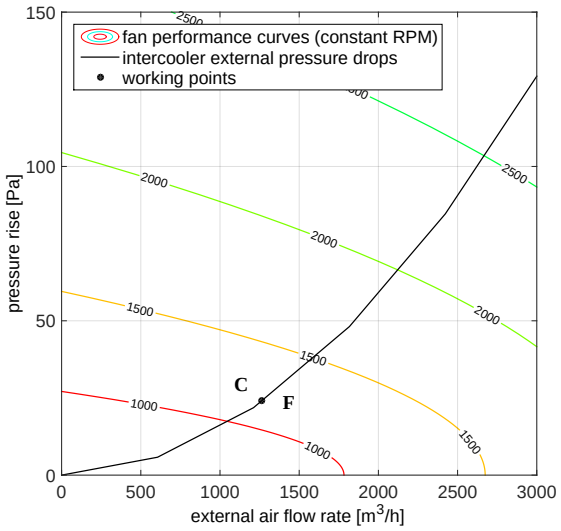


Figure 9: Fan performance map and operating points in simulation cases C and F

of the dual stage concept, the intercooler is not advisable.

6. Conclusions

The current research compared the performance of single and dual stage sliding vane compressors layout with conventional and innovative injection technologies. The split of the compression process in two phases revealed that:

- indicated power savings up to 15%;
- an intercooling heat exchanger would not provide additional benefits;
- less energy is required to pressurize the oil;
- oil spray injection would not be as effective as occurs in single stage compressors;
- lower mechanical efficiencies are expected because of greater overall friction losses.

If all these phenomena are taken into account, a dual stage compressor system might potentially lead to overall electrical savings up to 9.5%.

The economic feasibility of the solution outlined essentially depends on the utilization factor of the compressor system, on the cost of electricity and on the carbon tax. All these parameters have geographical spreads that do not allow to perform accurate predictions yet. However, in order to take into account also the additional maintenance costs due to a more complex compressor system, further investigations are going to be performed thanks to experiments on a real prototype.

7. Acknowledgment

The work has been done under the FP7 Project "Complete Vehicle Energy-Saving CONVENIENT" funded by the European Commission.

References

[1] Saidur R, Rahim N and Hasanuzzaman M 2010 *Renewable and Sustainable Energy Reviews* **14** 1135 – 1153 ISSN 1364-0321

[2] Radgen P 2001 *Compressed air systems in the European Union: energy, emissions, savings potential and policy actions* (LOG_X Verlag GmbH)
[3] European Association of Manufacturers of Compressors, Vacuum Pumps, Pneumatic Tools and Air and Condensate Treatment Equipment PNEUROP `www.pneurop.eu` last access: 2015-01-20
[4] Cipollone R 2014 *Proceedings of the Institution of Mechanical Engineers, Part E: Journal of Process Mechanical Engineering*
[5] Vittorini D, Bianchi G and Cipollone R in press *Energy Procedia*
[6] Badr O, O'Callaghan P and Probert S 1985 *Applied Energy* **19** 159 – 182 ISSN 0306-2619
[7] Wu J H, Zhang L, Huang L Q and Tang Y Y 2004 *Proceedings of the International Compressor Engineering Conference*
[8] Aradau D and Costiuc L 1996 *Proceedings of the International Compressor Engineering Conference*
[9] Badr O, Probert S and O'Callaghan P 1985 *Applied Energy* **20** 253 – 285 ISSN 0306-2619
[10] Reed W and Hamilton J 1980 *Proceedings of the International Compressor Engineering Conference*
[11] Fukuta M, Yanagisawa T and Shimizu T 1992 *Proceedings of the International Compressor Engineering Conference*
[12] Al-Hawaj O 2009 *International Journal of Refrigeration* **32** 1555 – 1562 ISSN 0140-7007
[13] Huang Y M and Yang S A 2008 *Measurement* **41** 835 – 841 ISSN 0263-2241
[14] Tramschek A and Mkumbwa M 1996 *Proceedings of the International Compressor Engineering Conference*
[15] Lee J, Lee U, Sung C, Han K and Kim E 2008 *Proceedings of the International Compressor Engineering Conference*
[16] Hirano K and Monasry J 2012 *Proceedings of the International Compressor Engineering Conference*
[17] Takashima K, Onoda I, Kitaichi S and Watanabe N 2004 *Proceedings of the International Compressor Engineering Conference*
[18] Valente R and Villante C 2008 *Proceedings of the 20th International Compressor Engineering Conference*
[19] Bianchi G and Cipollone R 2015 *Applied Energy* **142** 95 – 107 ISSN 0306-2619
[20] Bianchi G and Cipollone R 2015 *Applied Thermal Engineering* **84** 276 – 285 ISSN 1359-4311
[21] Cipollone R, Valenti G, Bianchi G, Murgia S, Contaldi G and Calvi T 2014 *Proceedings of the Institution of Mechanical Engineers, Part E: Journal of Process Mechanical Engineering*
[22] Bianchi G, Cipollone R, Murgia S and Contaldi G 2014 *Proceedings of the International Compressor Engineering Conference*
[23] Cipollone R, Bianchi G and Contaldi G 2012 *ASME 2012 International Mechanical Engineering Congress and Exposition* vol 6 pp 69 – 80 ISBN 978-0-7918-4522-6
[24] Bianchi G, Cipollone R, Murgia S and Contaldi G 2015 *International Journal of Refrigeration* **52** 11 – 20 ISSN 0140-7007
[25] Cipollone R, Battista D D and Gualtieri A 2013 *Energy Conversion and Management* **75** 581 – 592 ISSN 0196-8904

Nomenclature

α	fan coefficient $[m^3/s]$	C	turbulent coefficient $[-]$	$ad-is$	adiabatic-isentropic
γ	heat specific ratio $[-]$	D	diameter $[m]$	el	electrical
μ	dynamic viscosity $[Pa\,s]$	L	length $[m]$	ext	external
Δp	pressure drop $[Pa]$	N	revolution speed $[RPM]$	fr	friction
ρ	air density $[kg/m^3]$	Nu	Nusselt number $[-]$	$glob$	global
c_p	specific heat at const. p $[kJ/kg/K]$	P	power $[W]$	i	inlet
f_m	friction multiplier $[-]$	Pr	Prandtl number $[-]$	ind	indicated
h	heat transfer coefficient $[W/(m^2\,K)]$	Q	thermal power $[W]$	int	internal
k	thermal conductivity $[W/(m\,K)]$	R	thermal resistance $[K/W]$	j	discretization index
$\dot{m}$	mass flow rate $[kg/s]$	S	heat transfer surface $[m^2]$	$mech$	mechanical
n	Reynolds number exponent $[-]$	T	temperature $[K]$	o	outlet
p	pressure $[Pa]$	$\dot{V}$	volumetric flow rate $[m^3/s]$	org	organic
v	air flow speed $[m/s]$	1	first stage	ref	reference
A	cross sectional fluid area $[m^2]$	2	second stage	vol	volumetric